

Lattice study of QCD at finite chiral density: topology and confinement

N. Yu. Astrakhantsev,^{1,2,3} V. V. Braguta,^{1,2,3,4} A. Yu. Kotov,^{1,2,3,*} and A. A. Nikolaev^{2,5}

¹ *Moscow Institute of Physics and Technology, Institutsky lane 9, Dolgoprudny, Moscow region, 141700*

² *Institute for Theoretical and Experimental Physics NRC “Kurchatov Institute”, Moscow, 117218 Russia*

³ *Bogoliubov Laboratory of Theoretical Physics, Joint Institute for Nuclear Research, Dubna, 141980 Russia*

⁴ *Far Eastern Federal University, School of Biomedicine, 690950 Vladivostok, Russia*

⁵ *Department of Physics, College of Science, Swansea University, Swansea SA2 8PP, United Kingdom*

In this paper we study the properties of QCD at nonzero chiral density ρ_5 , which is introduced through chiral chemical potential μ_5 . The study is performed within lattice simulation of QCD with dynamical rooted staggered fermions. We first check that ρ_5 is generated at nonzero μ_5 and in the chiral limit observe $\rho_5 \sim \Lambda_{QCD}^2 \mu_5$. We also test the possible connection between confinement and topological fluctuations. To this end, we measured the topological susceptibility χ_{top} and string tension σ for various values of μ_5 . We observed that both string tension and chiral susceptibility grow with μ_5 and there is a strong correlation between these quantities. We thus conclude that the chiral chemical potential enhances topological fluctuations and that these fluctuations can indeed be closely related to the strength of confinement.

PACS numbers: 12.38.Gc, 12.38.Aw

Keywords: Lattice simulations of QCD, confinement, deconfinement, chiral chemical potential

I. INTRODUCTION

Quantum Chromodynamics (QCD) is believed to be the theory of strong interaction. While microscopic QCD Lagrangian is well known, the theory itself is extremely complicated and possesses a plenty of not fully understood nontrivial properties and phenomena. The most well-known examples include color confinement and chiral symmetry breaking.

One of the possible ways to shed light on these phenomena and their mechanism is to investigate QCD or QCD-like theories under extreme conditions. These extreme conditions include finite temperature studies [1–4], the influence of large magnetic field on QCD properties [5–9], QCD and QCD-like theories at finite baryon density [10–17] and QCD at finite isospin density [18].

Among others are the properties of QCD at nonzero chiral density. Systems with nonzero chiral density attract considerable attention because of unusual phenomena which take place in such systems. The renowned example of such phenomena is the chiral magnetic effect (CME) [19, 20], the appearance of electric current in chiral medium along applied magnetic field. Nonzero chiral density can be generated in heavy ion collisions either due to sphaleron transitions in quark-gluon plasma [21, 22] or due to the axial anomaly in parallel electric and magnetic fields [23]. There are a lot of studies of QCD properties with chiral density which is introduced through nonzero chiral chemical potential [24–35].

One of the interesting questions which can be addressed is how the confinement and the chiral symmetry breaking in QCD are affected by nonzero chiral density. The influence of nonzero chiral chemical potential on the chiral symmetry breaking was considered in a number of theoretical papers [24–28, 32, 35] as well as in the lattice studies [33, 34]. Today it is clear that in any system the chiral chemical potential either creates or enhances the dynamical chiral symmetry breaking depending on the strength of interactions between constituents in the media. This phenomenon was called the chiral catalysis and the mechanism responsible for this phenomenon was first explained in [35]. The essence of this phenomenon is that nonzero chiral density generates additional fermionic states which take part in the formation of the chiral condensate.

In this paper we mainly address three questions. First, we show that introduction of nonzero μ_5 to the system Hamiltonian leads to generation of nonzero chiral density ρ_5 . We study its dependence within lattice simulation of QCD and compare the observed behavior with the existing models such as ChPT and NJL. Second, we study the influence of chiral density on topological structure of QCD and show that topological susceptibility χ_{top} increases with chiral density ρ_5 . Finally, we study the confinement in QCD with nonzero μ_5 and its connection to the topology of QCD. The possible link between these phenomena was introduced in [36, 37]. Namely, the authors suggested to modify

*Corresponding author: andrey.kotov@phystech.edu

the gluon propagator to have the form $G(p) = (p^2 + \chi_{\text{top}}/p^2)^{-1}$ due to Veneziano ghosts tunnelling between different topological sectors of QCD. This form of gluon propagator implies maximum propagation range of order $\chi_{\text{top}}^{-1/4}$ and suggests enhancement of confinement with the growth of topological susceptibility. To check this connection, we study the string tension σ between heavy quark and antiquark at nonzero μ_5 and its correlation with topological susceptibility χ_{top} . Our results support the idea that topological properties and confinement are tightly connected.

It is well known that introduction of baryon chemical potential leads to the sign problem in $SU(3)$ theory and spoils the LQCD simulations. On contrary, introduction of the chiral chemical potential does not lead to the sign problem [19], which allows us to carry out this study within lattice simulation of QCD.

This paper is organized as follows. In the next section we discuss the chiral density generated by nonzero chiral chemical potential in QCD. In the section III we describe the details of our lattice simulation. Our results are presented in the section IV. In the last section we discuss our results and draw the conclusions. In Appendix A we derive the chiral density for free "naive" fermions and study divergences in the chiral density.

II. NONZERO CHIRAL CHEMICAL POTENTIAL IN QCD

In this paper we are going to study the properties of QCD with nonzero chiral density $\rho_5 = \bar{\psi}\gamma_4\gamma_5\psi$. It is well known that nonzero baryon density can be introduced to statistical system through modification of the Hamiltonian in the partition function $\hat{H} \rightarrow \hat{H} - \mu \int d^3x \bar{\psi}\gamma_4\psi$.¹ Similarly, one can modify the Hamiltonian by the term with chiral chemical potential μ_5

$$\hat{H} \rightarrow \hat{H} - \mu_5 \int d^3x \bar{\psi}\gamma_4\gamma_5\psi. \quad (1)$$

We would like to stress that the chiral chemical potential is different to the baryon chemical potential since chiral density is not conserved. There are two operators resulting in the non-conservation of the chiral density

$$\frac{d}{dt} \int d^3x \rho_5 = \frac{\alpha_s N_c}{4\pi} \int d^3x F_{\mu\nu}^a \tilde{F}_{\mu\nu}^a + 2m \int d^3x \bar{\psi}\gamma_5\psi. \quad (2)$$

The first operator $\sim F_{\mu\nu}^a \tilde{F}_{\mu\nu}^a$ is the anomalous contribution due to quantum corrections. The second operator $\sim m\bar{\psi}\gamma_5\psi$ results from the equation of motion for massive fermions. Note that chirality is not well-defined for massive fermions due to the possible spin flipping process. The dynamical fermion mass generation $\sim \Lambda_{QCD}$ due to the chiral symmetry breaking can significantly increase the effect of spin flipping. Thus, the physical meaning of modification (1) should be discussed more carefully. It is clear that the ρ_5 operator becomes the true chiral density only in the massless limit $\rho_5|_{m \rightarrow 0} = (Q_R - Q_L)/V$. For massive quarks the meaning of the ρ_5 operator should be considered in more detail.

Chemical potential is usually introduced with respect to conserved charge. In our study we consider $\mu_5\rho_5$ as the new term in the Hamiltonian and the conservation of ρ_5 is not required. We expect that the modification (1) leads to nonzero averaged value of the chiral density operator $\langle\rho_5\rangle \neq 0$ even for nonzero quark mass. The situation with μ_5 and ρ_5 is similar to the one with the fermion mass term $m\bar{\psi}\psi$. The conservation of the $\bar{\psi}\psi$ operator is not required and once this operator is introduced to the Hamiltonian it leads to the generation of nonzero condensate $\langle\bar{\psi}\psi\rangle \neq 0$. To show that it is very likely that non-zero μ_5 will result in non-zero ρ_5 generation even at finite quark mass, let us consider various models of QCD.

First, in terms of fermionic spectrum, the modification of the Hamiltonian (1) modifies the dispersion relation $E^2(p) = (|\vec{p}| - s\mu_5)^2 + m^2$ [24], where $s = \pm 1$ is the fermion helicity. For $\mu_5 > 0$ this implies that at fixed momentum $|\vec{p}|$ the fermion with helicity $s = +1$ has smaller energy than the one with $s = -1$. In thermodynamic equilibrium there will be a larger number of fermions with helicity $s = +1$ than that with $s = -1$. So one can expect that the modification (1) leads to nonzero helicity even at nonzero quark mass.

We proceed with the consideration of $SU(N_c)$ QCD with finite chemical potential in the large N_c limit $N_c \rightarrow \infty$. At low temperature T the chiral perturbation theory (ChPT) [38, 39] can be applied. In the leading order in $1/N_c$ there is no contribution of the anomalous term. Modification (1) only adds the flavour singlet axial current $A_\mu = \mu_5\delta_{\mu 4}\hat{1}$ and the modification of the partition function due to the introduction of this axial current within ChPT reads

$$Z(\mu_5) = Z_{QCD} \times \exp(\beta V N_f f_\pi^2 \mu_5^2), \quad \beta = \frac{1}{T}. \quad (3)$$

¹ In this paper we study QCD in thermodynamic equilibrium. So, instead of real time one has Euclidean time which is designated as a fourth component of four-vector. In particular, we use the following notation $\gamma_4 = \gamma_0$

From Eq. (3) it is seen that nonzero μ_5 leads to the additional constant factor in the QCD partition function, i.e. it is not related to dynamical degrees of freedom of the ChPT. This is because the ChPT accounts the chiral symmetry breaking in QCD but it does not provide its mechanism. In more complicated models [40, 41] which consider the chiral symmetry breaking mechanism, the μ_5 couples to the scalar σ and η' fields, which leads to enhancement of the chiral symmetry breaking with μ_5 and the chiral catalysis phenomenon in QCD [35].

From (3) for two flavor QCD one has

$$\langle \rho_5 \rangle = \frac{1}{\beta V} \frac{\partial \log Z(\mu_5)}{\partial \mu_5} = 4f_\pi^2 \mu_5. \quad (4)$$

So, one can see that the modification of the Hamiltonian (1) indeed leads to nonzero $\langle \rho_5 \rangle$ in the limit $N_c \rightarrow \infty$ even at nonzero quark mass.

Similar study can be carried out in the Nambu-Jona-Lasinio (NJL) model [42], which successfully describes low energy phenomenology of QCD. Since the NJL model is usually studied within the saddle point approximation, a lot of results are obtained within the $N_c \rightarrow \infty$ assumption. Within the NJL model, the chiral symmetry breaking leads to the generation of the dynamical quark mass $m \sim \Lambda_{QCD}$. The calculation of the chiral density with the quark mass $m \sim \Lambda_{QCD}$ gives $\langle \rho_5 \rangle \sim \Lambda_{QCD}^2 \mu_5$ (see Appendix A). This is another argument in favor of the hypothesis that non-zero chiral density can be generated at finite mass $\langle \rho_5 \rangle \sim \Lambda_{QCD}^2 \mu_5 \neq 0$.

On the one hand the approximation $N_c \rightarrow \infty$ works quite well for real QCD. So, one might expect that $\langle \rho_5 \rangle \sim \Lambda_{QCD}^2 \mu_5 \neq 0$ for $N_c = 3$. However, the anomaly contribution which appears in higher orders $\sim 1/N_c$ -corrections can modify the $N_c \rightarrow \infty$ result for the chiral density. To clarify the $N_c = 3$ behavior in Section IV we conduct lattice study of chiral density ρ_5 at nonzero chiral chemical potential.

III. LATTICE SETUP

In this paper we are going to study QCD with two flavours and nonzero chiral chemical potential. To this end we perform lattice simulations with the $SU(3)$ gauge group and employed the tree level improved Symanzik gauge action [43, 44]. For the fermionic part of the action we used staggered fermions with the action [34]

$$S_f = ma \sum_x \bar{\psi}_x \psi_x + \frac{1}{2} \sum_{x\mu} \eta_\mu(x) (\bar{\psi}_{x+\mu} U_\mu(x) \psi_x - \bar{\psi}_x U_\mu^\dagger(x) \psi_{x+\mu}) + \frac{1}{2} \mu_5 a \sum_x s(x) (\bar{\psi}_{x+\delta} \bar{U}_{x+\delta,x} \psi_x - \bar{\psi}_x \bar{U}_{x+\delta,x}^\dagger \psi_{x+\delta}), \quad (5)$$

where the $\eta_\mu(x)$ are the standard staggered phase factors: $\eta_1(x) = 1, \eta_\mu(x) = (-1)^{x_1 + \dots + x_{\mu-1}}$ for $\mu = 2, 3, 4$. The lattice spacing is denoted by a , the bare fermion mass by m , and μ_5 is the chiral chemical potential. In the chirality breaking term $s(x) = (-1)^{x_2}$, $\delta = (1, 1, 1, 0)$ represents a shift to the diagonally opposite site in a spatial 2^3 elementary cube. The combination of three links connecting sites x and $x + \delta$,

$$\bar{U}_{x+\delta,x} = \frac{1}{6} \sum_{i,j,k=\text{perm}(1,2,3)} U_i(x + e_j + e_k) U_j(x + e_k) U_k(x) \quad (6)$$

is symmetrized over the 6 shortest paths between these sites. In the partition function, after integrating out fermions, one obtains the corresponding fermionic determinant. In order to obtain two flavours in the continuum limit we apply the rooting procedure.

In the continuum limit and after rooting procedure our lattice action can be rewritten in the Dirac spinor-flavor basis [45, 46] as follows

$$S_f \rightarrow S_f^{(cont)} = \int d^4x \sum_{i=1}^2 \bar{q}_i (\partial_\mu \gamma_\mu + ig A_\mu \gamma_\mu + m + \mu_5 \gamma_5 \gamma_4) q_i. \quad (7)$$

We would like to emphasize that the chiral chemical potential introduced in Eq. (5) corresponds to the taste-singlet operator $\gamma_5 \gamma_4 \otimes \mathbf{1}$ in the continuum limit.

It should be also noted here that the baryonic chemical potential [47] and the chiral chemical potential as in [48], are introduced to the action as the modification of the temporal links by the corresponding exponential factors in order to eliminate chemical-potential dependent quadratic divergences. For staggered fermions with the baryonic chemical

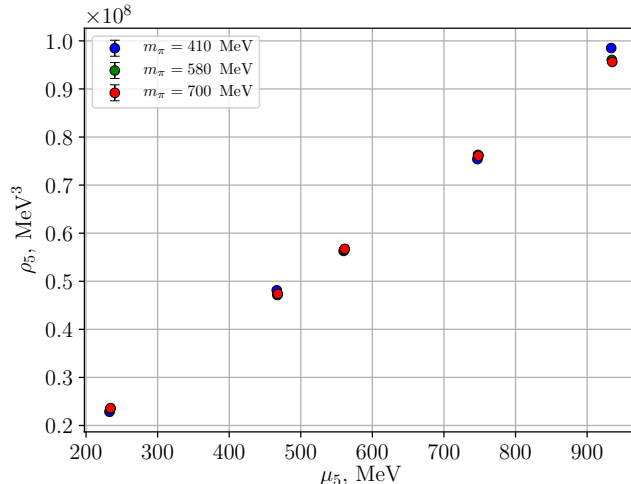


Figure 1: The chiral densities as a function of the chiral chemical potential for different pion masses and $a = 0.105$ fm.

potential this modification can be performed. However, in the case of μ_5 this method would lead to a highly non-local action [48]. Therefore, we introduce μ_5 in Eq. (5) in the additive way similarly to the mass term. It is known that the additive introduction of the chemical potential might lead to additional divergences in observables. In this paper we perform lattice measurement of chiral density and gluonic observables: the topological charge, the topological susceptibility and the string tension. In what follows we account ultraviolet divergences in the chiral density. We also believe that there are no additional divergences due to chiral chemical potential in gluon observables, because the chiral chemical potential term can be considered as some vertex with coupling constant of dimension of energy. It is known that the inclusion of such vertex to Feynman diagrams reduces the power of ultraviolet divergences. Since the fermion loops in QCD diverge as powers of $\log a$, the chiral chemical potential does not give rise to additional divergences. The ultraviolet divergences in QCD with chiral chemical potential are also discussed in [33, 34].

In the calculation we employed three different lattices with different lattice spacings to keep the physical volume fixed at approximately 1.7 fm^3 : 14^4 with $a = 0.128(3) \text{ fm}$ ($\beta = 3.9$), 16^4 with $a = 0.1054(11) \text{ fm}$ ($\beta = 4.0$) and 20^4 with $a = 0.0856(14) \text{ fm}$ ($\beta = 4.1$). To investigate chiral properties for each of the listed lattices three values of pion mass were considered: $m_\pi = 410, 580, 700 \text{ MeV}$. We note that the simulations performed in this paper indicate that the required simulation time grows with the chiral chemical potential. Lattice simulations at the largest values of chiral chemical potential are numerically very expensive.

IV. RESULTS OF THE CALCULATION

A. The chiral density

In this section we perform lattice measurement of the chiral density ρ_5 for all lattice spacings and pion masses under study. The chiral densities as a function of the chiral chemical potential for different pion masses and $a = 0.105$ fm are shown in Fig. 1. The chiral densities for other lattice spacings look similar. For this reason we do not show them. From Fig. 1 one sees that the data are well described by the linear dependence. It turns out that the coefficient of this linear dependence can be mostly attributed to the ultraviolet divergence in ρ_5 . However, our data are rather accurate. The uncertainties of the calculation are $\sim 1\%$, for this reason we can extract the sub-leading terms on the background of leading ultraviolet divergence.

To proceed we need to know the structure of the divergences in ρ_5 . In Appendix A the study of the ultraviolet divergences in ρ_5 for free "naive" fermions is presented. In particular, it is shown that there are two ultraviolet divergences in the term linear in μ_5 . The leading divergence is quadratic and the next-to-leading divergence is logarithmic. Additionally, the linear in μ_5 term contains finite contribution. Finally higher terms in μ_5 expansion do not contain ultraviolet divergences.

In this paper we are going to use the following formula for ρ_5 which accounts for the results obtained in Appendix:

$$a^3 \rho_5 = (A_1 + a^2 B_1 + C_1 (ma)^2 + D_1 (ma)^2 \log(ma)^2) (a\mu_5) + E_1 (a\mu_5)^3. \quad (8)$$

The coefficients A_1 and D_1 parameterize quadratic and logarithmic divergences and E_1 parameterizes finite μ_5^3 contribution. The B_1 and C_1 coefficients account finite contributions to the term linear in μ_5 . Note that the coefficients in (8) do not coincide with that derived in Appendix A since our simulations are performed with the staggered fermions instead of "naive" fermions. It is also reasonable to expect that the one-loop coefficients are modified by the radiative corrections.

In addition to (8) we are going to use the expression with smaller number of parameters

$$a^3 \rho_5 = (A_2 + a^2 B_2 + (ma)^2 C_2) (a\mu_5) + E_2 (a\mu_5)^3. \quad (9)$$

The difference between equations (8) and (9) is that the logarithmic term proportional to D_1 is included to C_2 . Notice that the possible higher order radiative corrections to ρ_5 are included to the coefficients C_2 and E_2 . We believe that this approximation should work rather well since the coefficients C_2 and E_2 parameterize sub-leading terms and the logarithm is a slowly varying function.

Further we fit our data for all lattice spacings and pion masses by formulas (8) and (9). Considering the good accuracy of the ρ_5 measurement we believe that both fits describe our data quite well ($\chi^2/dof \sim 3$), and the fit parameters are listed in Table I.

formula	$A \times 10^{-2}$	$B, \text{MeV}^2 \times 10^2$	C	D	$E \times 10^{-3}$
(8)	2.84 ± 0.05	8.5 ± 1.9	-0.055 ± 0.36	-0.025 ± 0.06	2.35 ± 0.15
(9)	2.84 ± 0.04	8.7 ± 1.7	0.09 ± 0.03	—	2.4 ± 0.15

Table I: The results of the fit of lattice data for the ρ_5 by formulas (8) and (9).

It is important to notice that the coefficient B_1 from formula (8) and the coefficient B_2 from formula (9) are non-zero and $B_1 \sim B_2 \sim 900 \text{ MeV}^2$. These coefficients parameterize the chiral density in the continuum and in the chiral limits. For this reason we can state that $B_1, B_2 \sim \Lambda_{QCD}^2$ or $\rho_5 \sim \Lambda_{QCD}^2 \mu_5$. Notice, however, that it is not possible to write exactly $\rho_5 = B_1 \mu_5$ or $\rho_5 = B_2 \mu_5$ since multiplicative renormalization of ρ_5 might be important but goes beyond the scope of this paper. To summarize, the results of this section allow us to state that finite μ_5 generates nonzero chiral density $\rho_5 \sim \Lambda_{QCD}^2 \mu_5 + O(\mu_5^3)$.

B. The topological charge and topological susceptibility

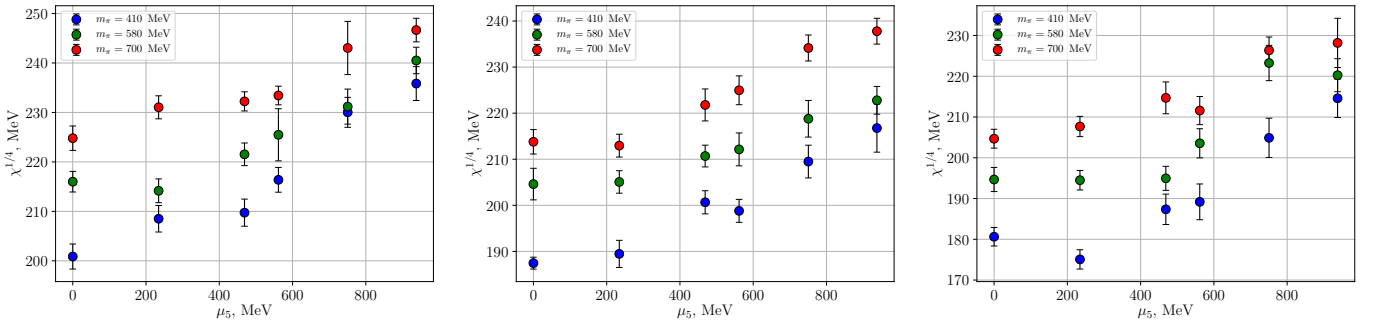


Figure 2: The topological susceptibilities as the functions of the chiral chemical potential for different pion masses and three different values of lattice spacing: $a = 0.128 \text{ fm}$, $a = 0.1054 \text{ fm}$, $a = 0.0856 \text{ fm}$ (from left to right).

Our next task is to study how nonzero chiral chemical potential influences the topological properties of QCD. To this end we measure the topological charge $\langle Q \rangle$ and the topological susceptibility $\langle Q^2 \rangle$ for different values of the chiral chemical potential under study.

Our measurement of the topological charge and the topological susceptibility mainly follows [49]. We smoothen each configuration using the Gradient Flow [50, 51]. Topological charge is measured on the smoothened configurations

$$Q_L = -\frac{1}{512\pi^2} \sum_x \sum_{\mu\nu\rho\sigma=\pm 1}^{\pm 4} \tilde{\epsilon}_{\mu\nu\rho\sigma} \text{Tr} U_{\mu\nu}(x) U_{\rho\sigma}(x), \quad (10)$$

where $U_{\mu\nu}(x)$ is the plaquette at the point x in directions μ and ν . In order to reduce the lattice artifacts we used the following estimators of the topological charge Q :

$$Q = \text{round}(\alpha Q_L), \quad (11)$$

where round gives the closest integer to its argument and the factor α is chosen in such a way that it minimizes

$$\langle (\alpha Q_L - \text{round}(\alpha Q_L))^2 \rangle. \quad (12)$$

In other words, we rescale our definition of the topological charge Q_L so that its peaks become closer to integer values and then round the result to this integer value. The topological susceptibility is then defined as

$$\chi_{\text{top}} = \frac{\langle Q^2 \rangle}{V_4}, \quad (13)$$

where V_4 is the four-dimensional volume of the lattice. We have found that for Gradient Flow times $t/a^2 > 3.0$ the dependence of the topological susceptibility χ_{top} on the value of Gradient Flow time exhibits a plateau with almost no dependence on the value of t . The value at this plateau was taken as a final estimation for the topological susceptibility χ_{top} .

Our results for the topological properties of QCD are the following. The topological charge is zero within the uncertainty of the calculations for all pion masses, lattice spacings and chiral chemical potentials under study.

The topological susceptibilities as the functions of the chiral chemical potential for different pion masses and three different values of lattice spacing $a = 0.128 \text{ fm}$, $a = 0.1054 \text{ fm}$, $a = 0.0856 \text{ fm}$ are shown in Fig. 2.

Unfortunately our data do not allow us to take the continuum limit. To do this we need more data points for smaller lattice spacings and even better accuracy. Lattice simulations with smaller lattice spacing and nonzero chiral chemical potential require quite large numerical resources which are currently unavailable. However, from Fig. 2 one sees that the chiral chemical potential indeed enhances the topological fluctuations in QCD for all pion masses and lattice spacings under study. For this reason, we believe that the chiral chemical potential enhances the topological fluctuations in QCD in the continuum limit.

We believe that this observation can be understood as follows. The chiral density is a part of the chiral anomaly which implies that the change of ρ_5 can create nonzero topological charge. For this reason one can expect that the fluctuations in the chiral density lead to the fluctuations in the topological charge due to the axial anomaly. Larger chiral density generated by larger μ_5 leads to larger fluctuations of the chiral density and due to the anomaly leads to larger topological fluctuations in QCD. Our results imply that μ_5 is the parameter which allows influencing the topological sector of QCD through the anomaly equation.

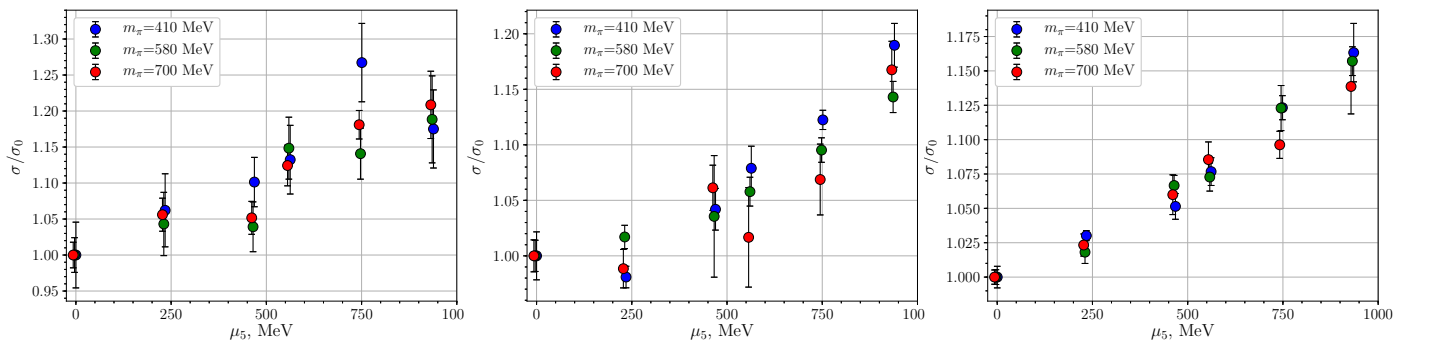


Figure 3: The ratios of the string tension σ to the string tension at zero chiral chemical potential σ_0 for three different values of lattice spacings $a = 0.128 \text{ fm}$, $a = 0.1054 \text{ fm}$, $a = 0.0856 \text{ fm}$ (from left to right). Points for different pion masses are slightly shifted in horizontal axis for better visibility.

C. The string tension

In order to study how nonzero chiral density influences the confinement properties of QCD we calculated the interaction potential of static charges through the measurement of Wilson loops. To obtain reasonable signal-to-noise ratio for Wilson loops the smearing techniques were employed. One step of the hypercubic blocking [52] with parameters $\alpha = (1.0, 1.0, 0.5)$ [53] was performed for the temporal links only, followed by 24 steps of the APE smearing [54] with $\alpha_{APE} = 0.165$.

The quark-antiquark interaction potential is related to Wilson loops as

$$V(R) = \lim_{t \rightarrow \infty} \log \left[\frac{\langle W(R, t) \rangle}{\langle W(R, t+1) \rangle} \right]. \quad (14)$$

This logarithm exhibits a clear plateau at large times $t/a \in [5; 9]$, its height was extracted as $V(R)$.

String tension σ was obtained from fitting the potential in the range $R \in [3.5a; L_s/2]$ by the Cornell fit

$$V(R) = A - \alpha/R + \sigma R. \quad (15)$$

This fit provides $\chi^2/dof \lesssim 1$ for all values of chiral chemical potentials. To estimate systematic uncertainty the left fitting range was varied in the interval $[3a; 4a]$ and the produced small change of $\sim 0.5\%$ in the string tension was added to the statistical error. Change of the right boundary of R in the fit does not alter the results in a noticeable way. Statistical errors for the fit parameters were estimated with the jackknife method.

The ratios of the string tension σ to the string tension at zero chiral chemical potential σ_0 for three different values of lattice spacings $a = 0.128$ fm, $a = 0.1054$ fm, $a = 0.0856$ fm are presented in Fig. 3. Unfortunately the continuum extrapolation of our results can not be performed because of quite large uncertainties. However, it is seen from Fig. 3 that the string tension rises with the chiral chemical potential i.e. with the chiral density. This is especially well seen at the smallest lattice spacing $a = 0.0856$ fm.

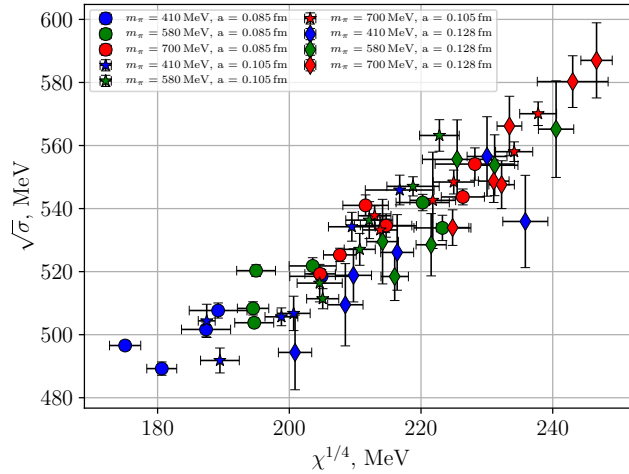


Figure 4: String tension $\sqrt{\sigma}$ as the function of chiral susceptibility $\chi_{\text{top}}^{1/4}$ for all values of pion mass and lattice spacing under study.

D. Topological fluctuations and confinement

The phenomenon of the QCD confinement is not well understood on the present day. However, papers [36, 37] have established a possible link between confinement properties and QCD topology. In their setup, gluon propagator is modified by the interaction with Veneziano ghosts tunneling between different topological sectors. The gluon propagator then reads $G(p) = (p^2 + \chi_{\text{top}}/p^2)^{-1}$, where χ_{top} is the topological susceptibility. The propagator has only complex poles $p^2 = \pm i\chi_{\text{top}}^{1/2}$, thus gluons cannot propagate as free particles. The typical range of gluon propagation

decreases as $\chi_{\text{top}}^{-1/4}$ with the growth of topological susceptibility. As one can observe from (section IV B) the topological susceptibility is enhanced by μ_5 . Thus, the confining properties, namely the string tension should also be enhanced by μ_5 and this is exactly our observation.

To further investigate this link, we put both $\chi_{\text{top}}^{1/4}$ and string tension $\sqrt{\sigma}$ on the same plot since we expect strong correlation between these quantities. In Fig. 4 we plot our data for all pion masses and lattice spacings in physical units. It is clearly seen that the string tension and topological susceptibility are correlated, though due to the smallness of relative change of these quantities the exact shape of this dependence (e.g. linear or quadratic) is unknown. This observation may be interpreted as an argument in favor of the mechanism presented in [36, 37].

V. CONCLUSION AND DISCUSSION

In this paper we studied the properties of QCD at nonzero chiral density ρ_5 , which is introduced through the chiral chemical potential μ_5 . Contrary to the baryon chemical potential introduction of the chiral chemical potential does not lead to the sign problem. For this reason our study of QCD with nonzero chemical potential can be performed within lattice simulation. In the simulations we employed the tree level improved Symanzik gauge action and rooted staggered fermions which in the continuum limit correspond to $N_f = 2$ dynamical quarks.

In the calculation we employed three different lattices with different lattice spacings to keep the physical volume fixed at approximately 1.7 fm^3 : 14^4 with $a = 0.128(3) \text{ fm}$ ($\beta = 3.9$), 16^4 with $a = 0.1054(11) \text{ fm}$ ($\beta = 4.0$) and 20^4 with $a = 0.0856(14) \text{ fm}$ ($\beta = 4.1$). To investigate the chiral properties for each of the listed lattices three values of pion mass were considered, $m_\pi = 410, 580, 700 \text{ MeV}$.

The first observable considered in this paper is the chiral density. We found that nonzero chiral chemical potential leads to generation of nonzero chiral density in QCD. Our lattice results support ChPT formula for the chiral density $\rho_5 \sim \Lambda_{QCD}^2 \mu_5$.

The next question is the influence of nonzero chiral chemical potential on the topological properties of QCD. To address this question we measured the topological charge and the topological susceptibility for various values of μ_5 . We found that the topological charge is zero for all values of the chiral chemical potential under investigation. On the contrary, we found that the topological susceptibility rises with μ_5 . So we conclude that the chiral chemical potential or chiral density enhance the topological fluctuations in QCD.

We believe that this observation can be understood as follows. Note that the chiral density enters the chiral anomaly which implies that the change of ρ_5 can generate nonzero topological charge. For this reason one can expect that the fluctuations of the chiral density lead to the fluctuations in the topological charge due to the axial anomaly. Larger chiral density generated by larger μ_5 leads to larger fluctuations of the chiral density and, due to the anomaly, to larger topological fluctuations in QCD.

The last observable studied in this paper is the string tension. We calculated the static potential from Wilson loops and determined the string tension for all values of chiral chemical potentials at lattice parameters studied. We found that the string tension rises with rising chiral chemical potential.

It would be interesting to understand the mechanism how confinement in QCD is enhanced by nonzero chiral chemical potential. One possible explanation can be based on the results of [36, 37], where the authors considered the gluon propagator, modified due to Veneziano ghosts tunneling between different topological sectors, making gluons confined at typical distances $\sim \chi_{\text{top}}^{-1/4}$ where χ_{top} is the topological susceptibility. As one can observe from (section IV B) the topological susceptibility is enhanced by μ_5 . Thus, the confining properties, namely the string tension should also be enhanced by μ_5 and this is exactly our observation.

Another possible explanation is that the gluon fields generated in the system due to fluctuations of ρ_5 might have nontrivial properties which give rise to the confinement. In particular, if the gluon fields are self-dual due to the ρ_5 fluctuations they might enhance the confinement [55–58]. Unfortunately, quite large uncertainties of the calculation do not allow us to draw any strong conclusion about the origin of confinement enhancement with μ_5 . This question including the mechanism of self-dual gluon fields is the subject for further research.

VI. ACKNOWLEDGMENTS

V. V. B. acknowledges the support from the BASIS foundation. The work of N. Yu. A. and A. Yu. K., which consisted of generation of configurations and measurement of topological susceptibility, string tension and chiral density, was supported by grant from the Russian Science Foundation (project number 18-72-00055). A. A. N. acknowledges the support from STFC via grant ST/P00055X/1. This work has been carried out using computing resources of the federal collective usage center Complex for Simulation and Data Processing for Mega-science Facilities at NRC “Kurchatov

Institute”, <http://ckp.nrcki.ru/>. In addition, the authors used the equipment of the shared research facilities of HPC computing resources at Lomonosov Moscow State University, the cluster of the Institute for Theoretical and Experimental Physics and the supercomputer of Joint Institute for Nuclear Research “Govorun”.

Appendix A: Ultraviolet divergences in the chiral density for free ”naive” fermions

To get an idea about the ultraviolet divergences in the chiral density at nonzero chiral chemical potential in this section we are going to derive the chiral density for free ”naive” fermions. The fermion propagator including the chiral chemical potential for ”naive” lattice fermions can be written in the following form

$$\begin{aligned}
S^{\alpha\beta}(x, y) &= \frac{\delta^{\alpha\beta}}{L_t L_s^3} \sum_{\{p\}} \sum_s e^{ip(x-y)} \frac{-i \sum_\mu \gamma_\mu \sin(p_\mu) + ma + (\mu_5 a) \gamma_4 \gamma_5}{\sin^2(p_4) + (|p| - s(\mu_5 a))^2 + (ma)^2} \times P(s), \\
P(s) &= \frac{1}{2} \left(1 - is \sum_i \frac{\gamma_i \sin(p_i)}{|p|} \gamma_0 \gamma_5 \right), \quad i = 1, 2, 3, \\
|p|^2 &= \sin^2(p_1) + \sin^2(p_2) + \sin^2(p_3), \\
p_i &= \frac{2\pi}{L_s} n_i, \quad i = 1, 2, 3, \quad n_i = 0, \dots, L_s - 1, \\
p_4 &= \frac{2\pi}{L_t} n_4 + \frac{\pi}{L_t}, \quad n_4 = 0, \dots, L_t - 1.
\end{aligned} \tag{A1}$$

Here m and μ_5 are mass and chiral chemical potential in physical units, α, β are color indices, the sum is taken over all possible values of (n_1, n_2, n_3, n_4) , $s = \pm 1$ and a is a lattice spacing.

In the limit $L_s, L_t \rightarrow \infty$ the chiral density in lattice units for two fermion flavours can be written as

$$\langle \bar{\psi} \gamma_4 \gamma_5 \psi \rangle_{lat} = -\frac{3N_f}{16} Sp[\gamma_4 \gamma_5 S(x, x)] = -\frac{3}{4} \sum_{s=\pm 1} \int \frac{d^4 p}{(2\pi)^4} \frac{s|p| - \mu_5 a}{\sin^2 p_4 + (|p| - s(\mu_5 a))^2 + (ma)^2} \tag{A2}$$

It should be noted here that the factor 3 in the first equality is due to the sum over the fermion colors. Now let us expand the chiral density (A2) in powers of the chiral chemical potential. It turns out that it is sufficient to keep only two terms: $\sim \mu_5$ and $\sim \mu_5^3$. Higher order terms in this expansion do not contain ultraviolet divergences. The calculation of the integrals which appear in this expansion is rather cumbersome but straightforward. For this reason we don’t show the details of the calculation. We would like only to mention that the integrals which appear in the expansion of (A2) in μ_5 can be found in [59]. The resulting expression for the chiral density ρ_5 in physical units can be written in the following form

$$\begin{aligned}
\rho_5 &= \frac{1}{a^3} \langle \bar{\psi} \gamma_4 \gamma_5 \psi \rangle_{lat} = \mu_5 J_1 + \mu_5^3 J_2 + O(\mu_5^5) \\
J_1 &= -0.464800 \frac{1}{a^2} - \frac{3}{\pi^2} m^2 \log(ma)^2 + 0.807241 m^2 \\
J_2 &= 0.242419
\end{aligned} \tag{A3}$$

Now few comments are in order.

- From equation (A3) we notice that there are two divergences in the linear in the μ_5 term. The leading divergence is quadratic and the next-to-leading divergence is logarithmic.
- In addition to the divergences the linear in the μ_5 term contains finite contribution which is proportional to the fermion mass in the second power $\rho_5 \sim m^2 \mu_5$. Now recall that in Nambu-Jona-Lasinio model[42], which successfully describes low energy phenomenology of QCD, the chiral symmetry breaking leads to generation of the dynamical fermion mass $m \sim \Lambda_{QCD}$. For this reason one can expect that due to chiral symmetry breaking in QCD the renormalized $\rho_5 \sim \Lambda_{QCD}^2 \mu_5$. ChPT confirms this statement (see section II).
- Notice also that the logarithmic ultraviolet divergence is also possible in the μ_5^3 term. However, final result does not contain the logarithmic ultraviolet divergence.
- If one takes the chiral limit in formula (5), it is possible to get rid of logarithmic divergence as well as final term proportional to m^2 . Unfortunately it is not possible to get rid of the $1/a^2$ divergence which results from the

additive way of introducing the chiral chemical potential. In addition to the divergence the additive chemical potential modifies the coefficient in front of the μ_5^3 contribution. For free chiral fermions this coefficient is determined by Fermi distribution and for three colors and two flavours it is $\rho_5(\mu_5) = 2/\pi^2 \cdot \mu_5^3 \simeq 0.202642 \cdot \mu_5^3$ ([19]). Comparing this value with the J_2 in formula (A3) it is seen that lattice artificial contribution is rather small but it is present. In this paper we concentrate on the linear in μ_5 term, thus the fact that the coefficient of the μ_5^3 term is modified by lattice artifacts does not affect the results of this paper.

-
- [1] A. V. Smilga, Phys. Rept. **291**, 1 (1997), hep-ph/9612347.
 - [2] M. D'Elia, Nucl. Phys. **A982**, 99 (2019), 1809.10660.
 - [3] N. O. Agasian, M. S. Lukashov, and Yu. A. Simonov, Mod. Phys. Lett. **A31**, 1650222 (2016), 1610.01472.
 - [4] R. A. Abramchuk, Z. V. Khaidukov, and Yu. A. Simonov (2018), 1812.01998.
 - [5] J. O. Andersen, W. R. Naylor, and A. Tranberg, Rev. Mod. Phys. **88**, 025001 (2016), 1411.7176.
 - [6] D. Kharzeev, K. Landsteiner, A. Schmitt, and H.-U. Yee, Lect. Notes Phys. **871**, pp.1 (2013).
 - [7] M. D'Elia, PoS **LATTICE2014**, 020 (2015), 1502.06047.
 - [8] V. D. Orlovsky and Yu. A. Simonov, Phys. Rev. **D89**, 054012 (2014), 1311.1087.
 - [9] M. A. Andreichikov, V. D. Orlovsky, and Yu. A. Simonov, Phys. Rev. Lett. **110**, 162002 (2013), 1211.6568.
 - [10] S. Muroya, A. Nakamura, C. Nonaka, and T. Takaishi, Prog. Theor. Phys. **110**, 615 (2003), hep-lat/0306031.
 - [11] C. S. Fischer (2018), 1810.12938.
 - [12] M. A. Andreichikov, M. S. Lukashov, and Yu. A. Simonov, Int. J. Mod. Phys. **A33**, 1850043 (2018), 1707.04631.
 - [13] V. V. Braguta, E. M. Ilgenfritz, A. Yu. Kotov, A. V. Molochkov, and A. A. Nikolaev, Phys. Rev. **D94**, 114510 (2016), 1605.04090.
 - [14] V. G. Bornyakov, V. V. Braguta, E. M. Ilgenfritz, A. Yu. Kotov, A. V. Molochkov, and A. A. Nikolaev, JHEP **03**, 161 (2018), 1711.01869.
 - [15] N. Yu. Astrakhantsev, V. G. Bornyakov, V. V. Braguta, E. M. Ilgenfritz, A. Yu. Kotov, A. A. Nikolaev, and A. Rothkopf (2018), 1808.06466.
 - [16] T. Boz, O. Hajizadeh, A. Maas, and J.-I. Skullerud (2018), 1812.08517.
 - [17] S. Cotter, P. Giudice, S. Hands, and J.-I. Skullerud, Phys. Rev. **D87**, 034507 (2013), 1210.4496.
 - [18] B. B. Brandt, G. Endrodi, and S. Schmalzbauer, in *13th Conference on Quark Confinement and the Hadron Spectrum (Confinement XIII) Maynooth, Ireland, July 31-August 6, 2018* (2018), 1811.06004.
 - [19] K. Fukushima, D. E. Kharzeev, and H. J. Warringa, Phys. Rev. **D78**, 074033 (2008), 0808.3382.
 - [20] A. Vilenkin, Phys. Rev. **D22**, 3080 (1980).
 - [21] D. E. Kharzeev, L. D. McLerran, and H. J. Warringa, Nucl. Phys. **A803**, 227 (2008), 0711.0950.
 - [22] A. Yu. Kotov, JETP Lett. **108**, 352 (2018), [Pisma Zh. Eksp. Teor. Fiz.108,no.6,374(2018)].
 - [23] M. Ruggieri and G. X. Peng, Phys. Rev. **D93**, 094021 (2016), 1602.08994.
 - [24] R. Gatto and M. Ruggieri, Phys. Rev. **D85**, 054013 (2012), 1110.4904.
 - [25] M. N. Chernodub and A. S. Nedelin, Phys. Rev. **D83**, 105008 (2011), 1102.0188.
 - [26] A. A. Andrianov, D. Espriu, and X. Planells, Eur. Phys. J. **C73**, 2294 (2013), 1210.7712.
 - [27] A. A. Andrianov, D. Espriu, and X. Planells, Eur. Phys. J. **C74**, 2776 (2014), 1310.4416.
 - [28] L. Yu, H. Liu, and M. Huang, Phys. Rev. **D94**, 014026 (2016), 1511.03073.
 - [29] T. G. Khunjua, K. G. Klimenko, and R. N. Zhokhov, Phys. Rev. **D97**, 054036 (2018), 1710.09706.
 - [30] T. G. Khunjua, K. G. Klimenko, R. N. Zhokhov, and V. C. Zhukovsky, Phys. Rev. **D95**, 105010 (2017), 1704.01477.
 - [31] T. G. Khunjua, K. G. Klimenko, and R. N. Zhokhov, Phys. Rev. **D98**, 054030 (2018), 1804.01014.
 - [32] A. Andrianov, V. Andrianov, and D. Espriu, EPJ Web Conf. **138**, 01007 (2017).
 - [33] V. V. Braguta, E. M. Ilgenfritz, A. Yu. Kotov, B. Petersson, and S. A. Skinderev, Phys. Rev. **D93**, 034509 (2016), 1512.05873.
 - [34] V. V. Braguta, V. A. Goy, E. M. Ilgenfritz, A. Yu. Kotov, A. V. Molochkov, M. Muller-Preussker, and B. Petersson, JHEP **06**, 094 (2015), 1503.06670.
 - [35] V. V. Braguta and A. Yu. Kotov, Phys. Rev. **D93**, 105025 (2016), 1601.04957.
 - [36] D. E. Kharzeev and E. M. Levin, Phys. Rev. Lett. **114**, 242001 (2015), 1501.04622.
 - [37] D. E. Kharzeev, Int. J. Mod. Phys. **A31**, 1645023 (2016), 1509.00465.
 - [38] S. Scherer, Adv. Nucl. Phys. **27**, 277 (2003), hep-ph/0210398.
 - [39] G. Ecker, Lect. Notes Phys. **521**, 83 (1999), hep-ph/9805500.
 - [40] E. Witten, Annals Phys. **128**, 363 (1980).
 - [41] P. Di Vecchia and G. Veneziano, Nucl. Phys. **B171**, 253 (1980).
 - [42] S. P. Klevansky, Rev. Mod. Phys. **64**, 649 (1992).
 - [43] P. Weisz, Nucl. Phys. **B212**, 1 (1983).
 - [44] G. Curci, P. Menotti, and G. Paffuti, Phys. Lett. **130B**, 205 (1983), [Erratum: Phys. Lett.135B,516(1984)].
 - [45] H. Kluberg-Stern, A. Morel, O. Napoly, and B. Petersson, Nucl. Phys. **B220**, 447 (1983).
 - [46] I. Montvay and G. Münster, *Quantum fields on a lattice* (Cambridge University Press, 1994).

- [47] P. Hasenfratz and F. Karsch, Phys. Lett. **125B**, 308 (1983).
- [48] A. Yamamoto, Phys. Rev. **D84**, 114504 (2011), 1111.4681.
- [49] C. Bonati and M. D’Elia, Phys. Rev. **D89**, 105005 (2014), 1401.2441.
- [50] M. Luscher, Commun. Math. Phys. **293**, 899 (2010), 0907.5491.
- [51] M. Lscher, JHEP **08**, 071 (2010), [Erratum: JHEP03,092(2014)], 1006.4518.
- [52] A. Hasenfratz and F. Knechtli, Phys. Rev. **D64**, 034504 (2001), hep-lat/0103029.
- [53] M. Della Morte, A. Shindler, and R. Sommer, JHEP **08**, 051 (2005), hep-lat/0506008.
- [54] M. Albanese et al. (APE), Phys. Lett. **B192**, 163 (1987).
- [55] H. Leutwyler, Phys. Lett. **96B**, 154 (1980).
- [56] G. V. Efimov and S. N. Nedelko, Phys. Rev. **D51**, 176 (1995).
- [57] S. N. Nedelko and V. E. Voronin, Eur. Phys. J. **A51**, 45 (2015), 1403.0415.
- [58] S. N. Nedelko and V. E. Voronin, Phys. Rev. **D93**, 094010 (2016), 1603.01447.
- [59] S. Capitani, Phys. Rept. **382**, 113 (2003), hep-lat/0211036.